International Journal of Current Engineering and Technology
ISSN 2277 - 4106

Available at http://inpressco.com/category/ijcet

Research Article

Magneto-Dielectric and Electromagnetic Absorbing studies of Antimony Doped Nickel Ferrites

Erum Pervaiz[Å] and I.H.Gul[Å*]

[Å]Thermal Transport Laboratory (TTL), School of Chemical and Materials Engineering (SCME), National University of Sciences and Technology (NUST), H-12 Islamabad., PAKISTAN

Accepted 05 November 2013, Available online 01 December 2013, **Vol.3, No.5 (December 2013)**

Abstract

Antimony (Sb^{3+}) doped nickel ferrites ($NiSb_xFe_{2-x}O_4$) with x=0.0, 0.035, 0.065 and 0.1, have been synthesized by hydrothermal route using an autoclave at 160 ^{0}C for 12 hrs. AC conductivities for all the samples have been observed in the frequency range of 1MHz to 3 GHz, where AC conductivity increases due to the addition of antimony in nanocrystalline nickel ferrites. Electromagnetic properties were studied by measuring complex dielectric permittivity (ε), complex magnetic permeability (μ*) in the frequency range of 1 MHz to 3 GHz at room temperature using RF/impedance analyzer. Reflection losses (RL) were calculated for all the samples using permittivity and permeability measurements according to the transmission line theory. Maximum RL of -54dB was obtained for antimony doped nickel ferrite x=0.065 at 2.4 GHz with a band width of 1.2 GHz and decreases for high antimony concentration x=0.1 (-49dB). Low dielectric permittivity, high permeability and conductivity made this material a compatible option for single layered and multilayered chip inductors. While low RL values suggest nickel ferrite a possible candidate for electromagnetic absorption devices and radar absorbing material.*

Keywords: Antimony nano ferrite, Complex dielectric permittivity, Complex permeability, Reflection losses.

1. Introduction

Ferrites (spinel and hexagonal) have been considered as promising ceramic materials for the use in high frequency applications due to the inherent insulating and dielectric characteristics and capacity of absorbing electromagnetic waves to enhance electromagnetic interference suppression (EMIS) (V. G. Harris *et al*., 2009, R. Valenzuela *et al*., 2012). Spinel ferrite nanoparticles have been investigated since many years as good microwave absorbing materials due to their low dielectric and magnetic losses. In the class of spinel ferrites nickel nano ferrite and its derivatives like Ni-Zn (X. Feng *et al*., 2007), Ni-Al (I. H. Gul *et al*., 2012), Ni-Cu-Zn (S. Y. Tong *et al*., 2013) and Ni-Re (E. E. Sileo *et al.*, 2004) have been under consideration mostly due to high DC-electrical resistivity and low density, low permittivity losses and flexibility. Nickel ferrite in pure and in the form of composite with polymers are preferred as electromagnetic (EM) absorbing materials in high frequencies (HF) and ultra high frequencies (UHF) [S. M. abbas *et al*., 2007). Physical properties of all the class of spinel ferrites are largely based upon type and concentration of substituting cations, the way they occupy the crystal lattice, synthesis route, sintering temperature and sintering time (E. Pervaiz *et al*., 2013). Synthesis route, sintering behavior and cation substitution all thesis parameters directly influence the microstructure of prepared ferrites that define the properties and behaviors of prepared spinel ferrites (A. M. M. farea *et al*., 2008). Nickel ferrite is an inverse ferrimagnetic spinel ferrite with Ni^{2+} ions occupied at octahedral sub-lattices (B-sites) and Fe^{3+} ions occupied at tetrahedral (A-sites) and octahedral sub-lattices equally (K. S. Muthu *et al*., 2013). Doping of nickel ferrites with different divalent and trivalent cations imparts distinct electrical and magnetic properties characterized by shift of ions between two sub-lattices. Many researches are available on the synthesis and EM absorbing properties of nickel ferrites and its composites with different materials (Z. H. Yang *et al*., 2012, D. L. Zhao *et al*., 2009, Y. Yang *et al*., 2012). In all the studies two things are normally required for a material to become good EM/Microwave absorber. One is the matching thickness of the absorbing layer and second is the mechanical, thermal and chemical stability for the military use and stealth technologies (Y. J. Shin *et al*., 1993). Hexa-ferrites used for EM/microwave absorbing applications need thick absorbers to obtain a significant absorption of incident electromagnetic waves, while spinel ferrites with low thickness (~ 2mm) could possibly serve the purpose alone or with insulating polymers. (B. F. Zhao *et al*., 2013) have studied the microwave absorbing properties of $LiZnFe_2O_4$. (Ch.

*Corresponding author' Tel: 0092-51-90855206

Sujhata *et al*., 2013) have reported the influence of sintering temperature on EM absorbing ability of NiCuZn ferrite. (J. C. Aphesteguy *et al*., 2009) have reported a comparison of microwave absorbing capacity for NiZn and NiCuZn ferrite. (J. L. Xie et al., 2007) have reported that a NiCoZn ferrite with a thickness of 3 mm is sufficient to obtain reflection loss (RL) of -35 dB. Magneto-dielectric properties can be modified easily by adding only small quantity of the trivalent cations of larger radii thereby substituting at octahedral sites and shifting ions from B-sites to A-sites. The present work aimed at the study of electromagnetic absorbing behavior of nickel antimony ferrites prepared by hydrothermal route. We investigated the influence of Sb^{3+} ions concentration on complex permittivity (ε*), complex permeability (μ*) and EM absorbing properties in the frequency range of 1 MHz to 3 GHz based on the microstructure of the prepared ferrites. Up to our knowledge we are first to report the EM absorbing study of antimony nickel ferrites.

2. Experimental techniques

Antimony doped nickel ferrites $NiSb_xFe_{2-x}O_4$ (x=0.0-0.1) with step increment of x=0.035 have been prepared by hydrothermal rout employing a Teflon lined stainless steel autoclave at temperature of 160 ^{0}C. Detailed synthesis steps with structural and morphological analysis have been recently published in our previous work (E. Pervaiz *et al*., 2013). Phase formation, purity and structural analysis of antimony doped nickel ferrites was performed by powder X-ray diffraction technique at room temperature by CuKα (λ =1.5406 Å) radiation with 2-theta in the range of 20^0 to 80^0. All the structural parameters were calculated using the standard relations. Average crystallite sizes (D) have been calculated by Sherrer formula and also using W-H plots and found to be in the range of 14 nm to 21 nm ±2 nm (E. Pervaiz *et al*., 2013).

Pellets (10 mm in diameter and 1.8 mm thickness) of samples were used for measuring the complex permittivity (ε′, ε″) and dielectric loss tangent ($tan\delta$) by RF material/impedance analyzer (Agilent E4991A) The complex permeability (μ′, μ″) of nano ferrites were measured using toroidal shape disc with ~8mm inner diameter, 16mm outer diameter and 1.8 mm thickness with the 16454A and 16453A test fixtures, respectively. The test fixtures were used after open-short-load calibration.

3. Results and Discussion

3.1. AC conductivity analysis

As the electromagnetic absorbing properties are characterized by microstructure that in turn is based upon the conduction mechanism. To see the conduction behavior, AC conductivities have been calculated in the observed frequency range 1 MHz-3 GHz. AC conductivity (σ_{AC}) for all the samples of Sb^{3+} doped nickel ferrites have been presented in Fig. 1. σ_{AC} have been calculated using relation $\sigma_{AC}= 2\pi f\varepsilon^0\varepsilon' tan\delta$ (K. M. Batoo *et al*., 2009), from complex permittivity data. It can be observed from the figure that AC conductivity increases linearly with frequency showing small polarons responsible for conduction. AC-conductivity decreases for the sample with antimony concentration x=0.035 but increases for higher concentration of antimony. Increase of conductivity with increase in the concentration of doping cation can be explained by the grain size and porosity. Porosity decreases with increase in the doping cation concentration showing that surface area of grains (high conductivity) increases with decrease in the number of grain boundaries (high resistivity) that is a sound reason for increase in AC conductivity for higher concentration (x>0.035) antimony ferrites as shown in the inset of Fig. 1.

3.2 Complex permittivity/complex permeability analysis

In order to study the electromagnetic absorption properties of antimony doped nickel ferrites, magneto-dielectric parameters (ε^* and μ^*) were measured using RF impedance/material analyzer in the frequency range of 1 MHz to 3 GHz using solid disc and toroid shape discs of ~1.8 mm thickness. Where complex permittivity's and permeability's can be represented as $\varepsilon^*=\varepsilon'-j\varepsilon''$ and $\mu^*=\mu'-j\mu''$. Figs. 2 (a, b) shows the real (ε′) and imaginary parts (ε″) of complex permittivity at room temperature. It can be observed from the graphs that dielectric dispersion behavior exist for the nickel antimony ferrites in the frequency range of 1 MHz to 3 GHz in accordance with Koop's theory (C. G. Koops *et al*., 1951).

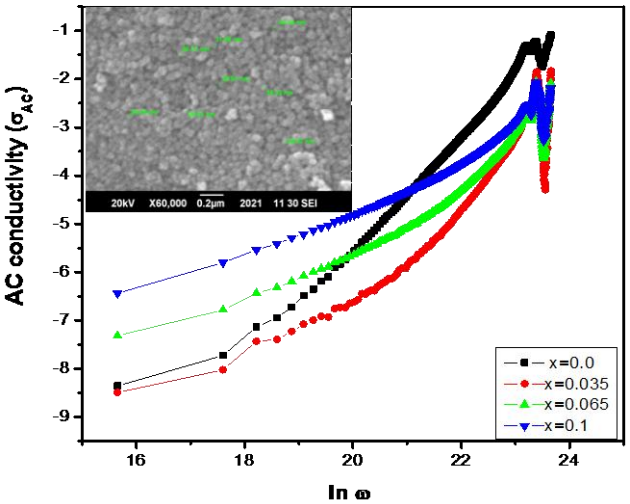

Fig. 1.Variation of AC conductivity σ_{AC} (1MHz-3 GHz) for $NiSb_xFe_{2-x}O_4$ (x=0.0-0.1) ferrite nanoparticles. (Inset) SEM image for $NiSb_xFe_{2-x}O_4$ (x=0.1)

Initially in low frequency range (MHz) there is a sudden decrease of dielectric permittivity (ε′) and losses (ε″) but as the frequency increases to GHz range, the value of both dielectric permittivity and losses becomes almost constant. Such kind of behavior is due to dielectric polarization (atomic and electronic) in the ferrites characteristics of microstructure (grain and grain boundaries) (A. Verma *et al*., 2011). From the graph it can be observed that

dielectric permittivity and losses are higher for pure nickel ferrites (x=0.0) but decreases for $x \geq 0.035$ in the low frequency region but concentration have almost no influence on dielectric permittivity and losses in high frequencies. Permittivity decreases for x=0.035 but increases for higher antimony concentration.

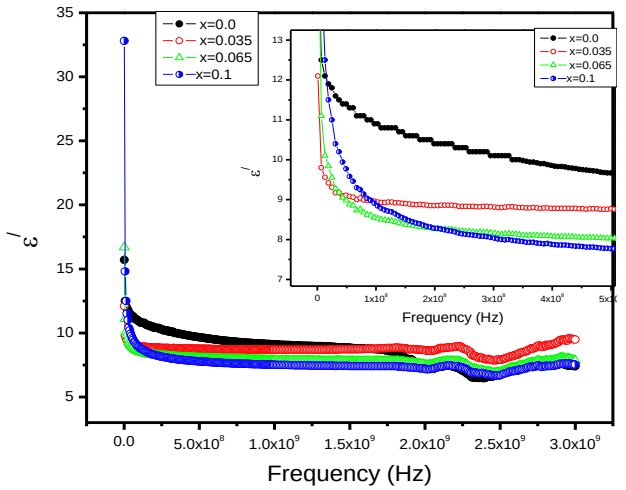

Fig. 2 (a) Variation of complex dielectric permittivity ε′ (real part) with f of $NiSb_xFe_{2-x}O_4$ (x=0.0-0.1) ferrite nanoparticles at room temperature

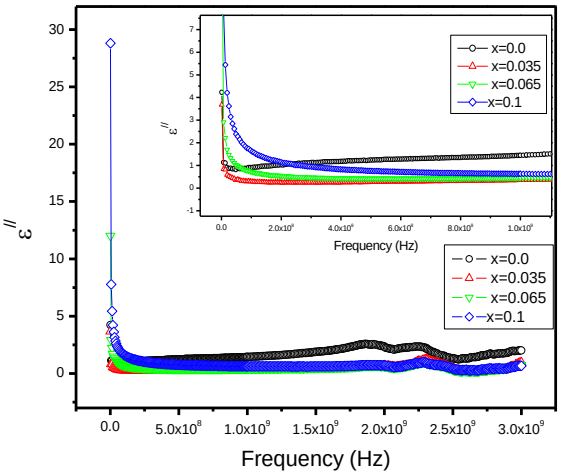

Fig. 2 (b) Variation of complex dielectric permittivity ε″ (imaginary part) with ln f of $NiSb_xFe_{2-x}O_4$ (x=0.0-0.1) ferrite nanoparticles

Figs. 3 (a, b) shows the behavior of real (μ') and imaginary parts (μ'') of complex permeability (magnetic characteristic) where μ'' represents the magnetic losses due to applied magnetic field. It can be observed from the graphs that both real and imaginary parts are constant for all the samples (x=0.0-0.1) in the entire frequency range except for the 2.6 GHz-3 G Hz, where a peak has been observed for all the samples. The reason for this peak is relaxation behavior in the said frequency range where domain wall rotation and applied AC field have resonance phenomenon. There is not a large difference but a slight decrease in the values of complex permeability due to increase in the antimony ions concentration.

Table 1 Dielectric permittivity real part (ε'), dielectric permittivity imaginary part (ε''), dielectric loss tangent ($tan\delta$), Magnetic permeability real part (μ'), Magnetic permeability imaginary part (μ''), Reflection loss (RL). Matching frequency (f_m) for $NiSb_xFe_{2-x}O_4$ (x=0.0-0.1)

Parameters	x=0.0	x=0.035	x=0.065	x=0.1
ε'(3 GHz)	7.39	9.48	7.83	7.53
ε''(3 GHz)	2.01	0.961	0.729	0.679
$\tan\delta_e$ (3 GHz)	0.0272	0.0101	0.0932	0.0902
μ'(3GHz)	26.8	15.6	15	16.1
μ''(3GHz)	19.2	-0.632	-0.657	-0.574
$\tan\delta_m$(3GHz)	0.0715	-0.04	-0.043	-0.0357
RL (dB)	-47	-43	-54	-49
f_m (GHz)	2.25	2.49	2.45	2.53

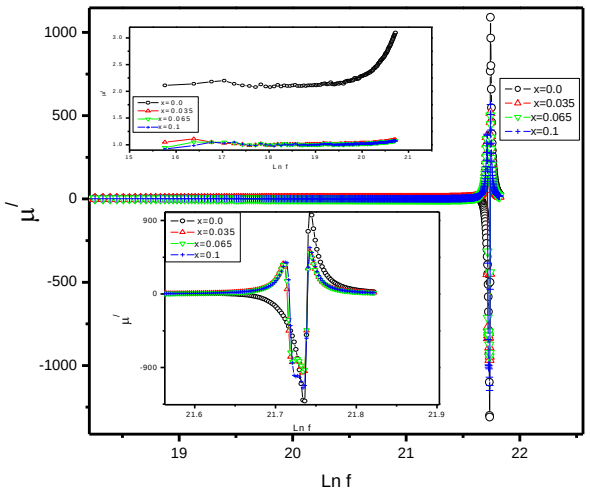

Fig. 3(a) Variation of complex magnetic permeability μ′ (real part) with ln f of $NiSb_xFe_{2-x}O_4$ (x=0.0-0.1) ferrite nanoparticles at room temperature.

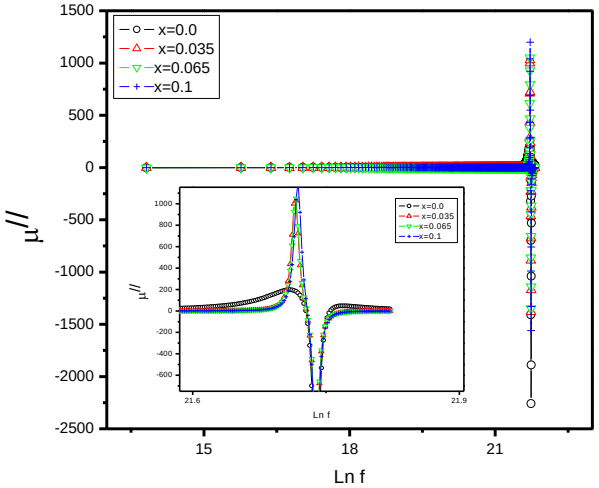

Fig. 3 (b) Variation of complex magnetic permeability μ″ (imaginary part) with f of $NiSb_xFe_{2-x}O_4$ (x=0.0-0.1) ferrite nanoparticles

The energy loss in spinel ferrites are associated with either dielectric nature or magnetic nature and represented by

$\tan\delta_e$ and $\tan\delta_m$ (H. M. Xiao *et al*., 2010). Dielectric loss tangent ($tan\delta_e = \varepsilon''/\varepsilon'$) and magnetic loss tangent ($tan\delta_m=\mu''/\mu'$) values decides about the nature of loss responsible for electromagnetic absorption in spinel ferrites. It can be observed from the Figs. 4 (a, b) that magnetic loss factor is constant and very minor for all the samples of nickel ferrites doped with antimony (x=0.0-0.1). Samples show significant dielectric losses in the range of (0.005-0.8). Dielectric loss factor decreases with increase in frequency.

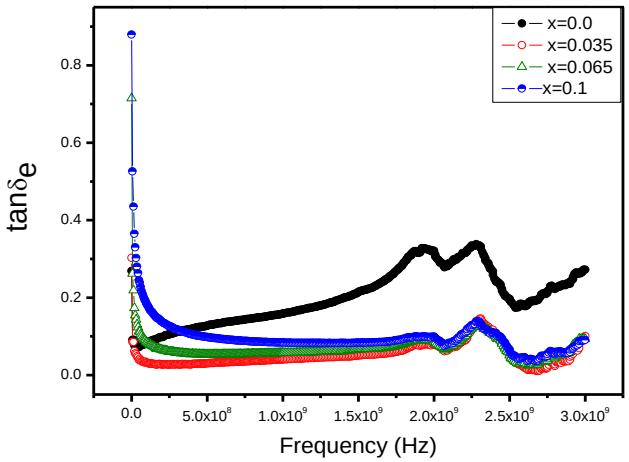

Fig. 4 (a) Variation of dielectric loss tangent ($\tan\delta_e$) with f

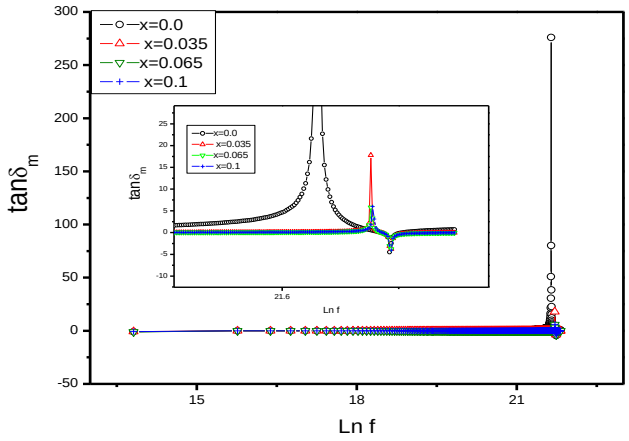

Fig. 4(b) Variation of magnetic loss tangent ($\tan\delta_m$) with f of $NiSb_xFe_{2-x}O_4$ (x=0.0-0.1) ferrite Nanoparticles

3.3 Electromagnetic absorbing analysis

Electromagnetic absorbing behavior has been studied from reflection loss (RL) measurements using coaxial line method of transmission line theory (J. Song *et al*., 2010). Reflection losses have been calculated using the following relations (Y. Naito *et al*., 1971) and represented in figure 5.

$$RL(dB) = 20Log_{10}\left|\frac{Z_{in}-1}{Z_{in}+1}\right| \quad (1)$$

$$Z_{in} = \sqrt{\frac{\mu^*}{\varepsilon^*}}\tanh(j2\pi ft/c \times \sqrt{\mu^*\varepsilon^*}) \quad (2)$$

where Z_{in} is the input impedance at the material-air interface, c is the speed of light, f is the frequency of incident waves and t is the thickness of absorbing layer. It can be observed from the graphs that all the samples show reflection loss of more than 90% (-10 dB) at matching thickness t_m of 1.8mm, in the given frequency range. The maximum reflection loss of -54 dB has been observed for x=0.065 at matching frequency (f_m) of 2.45 GHz. With increase in antimony ions concentration RL frequency shifts to higher side but a decrease in the value have been observed from -54 dB to -43 dB for x=0.1. As far as band gap is concerned, pure nickel ferrite has larger band width (1.94-2.39 GHz) which decreases for antimony doped ferrites. Such kind of RL behavior proves that antimony doped nickel ferrites can be applicable for electromagnetic absorption in high frequencies (~3 GHz).

4. Conclusions

Electromagnetic absorbing (EM) properties of all the samples of nano $NiSb_xFe_{2-x}O_4$ (x=0.0 to 0.1) with pure spinel phase prepared by hydrothermal route have been studied in the frequency range of 1MHz to 3 GHz. Complex permittivity have been observed to decrease with frequency but increases for maximum concentration of antimony (x=0.1). Complex permeability have been found to be independent in the whole frequency range where a relaxation peak have been observed around 2.5 GHz. Dielectric loss tangent contributes significantly towards electromagnetic absorption as compared to magnetic losses. Reflection losses (RL) were calculated for all the samples and it was observed that RL values lie in the range of -43 dB to -54 dB with increase in RL values by the increase in antimony concentration till x=0.065 (-54dB) and then decreases for x=0.1 (-43dB). RL peak shifts towards high frequency with increase in antimony ions concentration. High RL values describes that the EM absorption capacity of antimony doped nickel ferrites is much more than 90% (-10 dB) and such a material captures its attention for application at high frequencies.

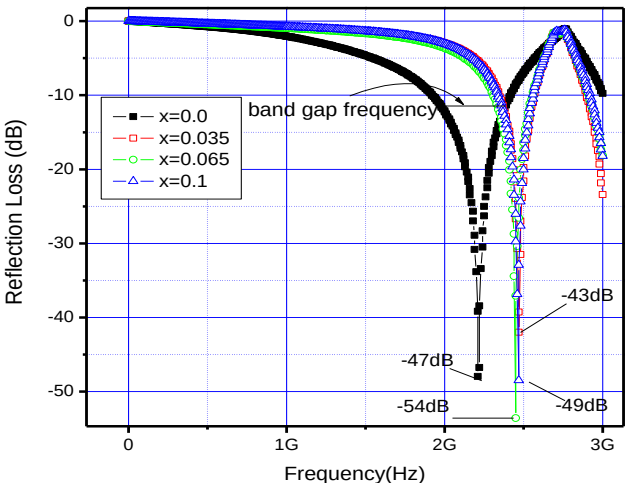

Fig. 5 Variation of Reflection losses (RL) with frequency for $NiSb_xFe_{2-x}O_4$ (x=0.0-0.1) ferrite nanoparticles

Acknowledgments

The authors would like to acknowledge NUST, TWAS, Italy, Higher Education Commission (HEC) Islamabad Pakistan project No.1326, for providing financial support for this work.

References

V.G. Harris, A. Geiler, Y. Chen, S. Daeyoon, M. Wu, A. Yang, Z. Chen, P. He, P.V. Parimi, Xu. Zuo, C.E. Patton, M. Abe, O. Acher, C. Vittoria (2009), *J. Magn. Magn. Mater*. Vol. 321, pp.2035–2047.

R. Valenzuela (2012), Novel application of soft ferrites, *Phys. Res. Inter*, Vol. 2012 , pp.1-9

X. Feng, Zhou Xiangchun, Li. Liangchao , Liu. Hui, Jiang Jing, Synthesis, Magnetic Properties and Microstructure of Ni-Zn-Cr Ferrites Doped with Lanthanum, *Journal of Rare earths*, 25, Suppl., (2007) 232.

I.H. Gul, E. Pervaiz (2012), Comparative study of NiAl ferrites prepared by chemical aco-precipitation and sol-gel auto combustion techniques, *Mater. Res. Bullt*. Vol. 47, pp.1353-1361.

S. Y. Tong, M. J. Tung, W. S. Ko, Yu. T. Huang, Y. P. Wang, Li. C. Wang, J. M. Wu (2013), Effect of Ni fillers on microwave absorption and effective permeability of NiCuZn ferrite/Ni/Polymer functional composites, *J. Alloy. Compds*. Vol. 550, pp.39-45.

E. E. Sileo, S. E. Jacobo (2004), Gadolinium-Nickel ferrites prepared from metal citrates precursors, *Physica. B*, Vol. 354, pp.241-245

S. M. Abbas, A. K. Dixit, R. Chatterjee, T.C. Goel (2007), Complex permittivity, complex permeability and microwave absorption properties of ferrite–polymer composites, *J. Magn. Magn. Mater*. Vol. 309, pp.20-24.

E. Pervaiz, I. H. Gul (2013), Low temperature synthesis and enhanced electrical properties by substitution of Al^{3+} and Cr^{3+} in Co-Ni nano ferrites, *J. Magn. Magn. Mater*. Vol. 343, pp.194-202.

A. M. M. Farea, S. Kumar, K. M. Batoo, A. Yousef, C.G. Lee, Alimuddin (2008), Structure and electrical properties of $Co_{0.5}Cd_xFe_{2.5-x}O_4$ ferrites, *J. Alloys. Compd*, Vol. 464, pp.361–369.

K. S. Muthu, N. Lakshminarasimhan (2013), Impedance spectroscopic studies of NiFe2O4 with different morphologies: microstructure vs. dielectric properties, *Ceram. Int*. Vol. 39, pp.2309-2315.

Z. H. Yang, Z. W. Li, L.B. Kong (2012), Enhanced microwave magnetic and attenuation properties of composites with free standing spinel ferrites thick films, *J. Magn. Magn. Mater*. Vol. 324, pp.3144-3148.

D. L. zhao, Q. L. Z. M. Shen (2009), Fabrication and microwave absorbing properties of NiZn spinel ferrites, *J. Alloys. Compd*, Vol. 480, pp.634-638.

Y. Yang, S. Qi, J. Wang (2012), Preparation and microwave absorbing properties of nickel-coated graphite nano sheet with pyrrole via in situ polymerization, *J. Alloys. Compd*, Vol. 520, pp.114-121.

J. Y. Shin, J. H. Oh (1993), The microwave absorbing phenomena of ferrite microwave absorbers, IEEE Trans. Magn. Vol. 29, pp.3437-3439.

B. F. Zhao, P. Ma, Ju-M. Zhao, Deng-Ao Li, X. Yang (2013), Fabrication and microwave absorbing properties of Li-Zn ferrite micro-belts/nickel coated carbon fibers composites, *Ceram. Int*. Vol. 39, pp.2317-2322.

Ch. Sujatha, K. V. Reddy, K. S. Babu, A. R. Reddy, K. H. Rao (2013), Effect of sintering temperature on electromagnetic properties of NiCuZn ferrite, *Ceram. Int*. Vol. 39, pp.3077-3086.

J. C. Aphesteguy, A. Damiani, D. Digiovanni, S. E. Jacobo (2009), Microwave absorbing characteristics of epoxy resin composites containing nanoparticles of NiZn and NiCuZn ferrites, *Phys. B*. Vol. 404, pp.2713-2716.

J. L. Xie, M. Han, L. Chen, R. Kuang, L. Deng (2007), Microwave-absorbing properties of NiCoZn spinel ferrites, *J. Magn. Magn. Mater*. Vol. 314, pp.37–42.

E. Pervaiz, I. H. Gul, A. Habib (2013), Hydrothermal Synthesis, Structural and Electrical Properties of Antimony ($Sb^{3+)}$ Substituted Nickel Ferrites, J Supercond. Nov. Magn. DOI: 10.1007/s10948-013-2364-4.

K. M. Batoo, S. Kumar, C. G. Lee, Alimuddin (2009), Study of AC impedance spectroscopy of Al doped $MnFe_{2-2x}Al_{2x}O_4$, *J. Alloys. Compd*, Vol. 480, pp.596-604.

C. G. Koop's (1951), On the dispersion of resistivity and dielectric constant of some semiconductors at audio frequencies**,** *Phys. Rev*, Vol. 83, pp.121-126.

A. Verma, O. P. Thakur, J. H. Hsu (2011), Temperature dependence of electrical properties of nickel-zinc ferrites processed by the citrate precursor technique, *J. Alloys. Compd*, Vol. 509, pp.5315-5321.

H. M. Xiao, W. D. Zhang, S. Y. Fu (2010), One-step synthesis, electromagnetic and microwave absorbing properties of α-FeOOH/polypyrrole nano-composites, *Comp. Sci. Tech*. Vol. 70, pp.909-915.

J. Song, L. Wang, X. Xu, N. C. Zhang (2010), Microwave electromagnetic and absorbing properties of Dy3+ doped MnZn ferrites, *J. Rar. Eart.* Vol. 28, pp. 451-458.

Y. Naito, K. Suetake (1971), Application of ferrite to electromagnetic wave absorber and its characteristics, IEEE Trans. MTT. Vol. 19, pp. 65-72.